Orbital Navigation using Resident Space Object Observations

Matt Driedger and Philip Ferguson
Department of Mechanical Engineering, University of Manitoba
E1-EITC 75 Chancellors Circle, Winnipeg, Manitoba, R3T 5V6
matt.driedger@umsats.ca
philip.ferguson@umanitoba.ca

ABSTRACT

With the population of Resident Space Objects (RSOs) in low earth orbit growing steadily year by year, there is an increasing challenge to track and map this population. While dedicated space and ground-based RSO detectors have done well, there has been an increasing amount of space-based detectors that assist in maintaining the RSO catalog. With continual RSO knowledge improvements, it may be possible to one day use RSO observations as a means of space-based navigation. This paper explores how this RSO information could one day be used in the attitude and orbit determination of the satellite. By leveraging the measurement parallax of nearby RSOs on the star tracker detector, the star tracker can be used to provide both orbit and attitude information to the navigation filter on-board the spacecraft, providing a useful backup to a standard GPS receiver. This paper presents preliminary work on a combined orbit / attitude Kalman filter that includes RSO observations from standard star trackers.

INTRODUCTION

Space exploration and the commercial use of space provides a demonstrated wealth of opportunities for academia and industry, ranging from basic physics research [1-5] to geology [6-9], security [10-13], agriculture [14-19], communications [20-23], astronomy [24-28], tourism [29-32] and even remote mining [33,34]. However, while humans have been exploiting space for more than half a century, many space companies have been slow to adopt new technologies, despite considerable advances by prominent Canadian and international space researchers [35-40]. Fear of the untested has resulted in a general industrial reluctance to incorporate modern engineering technologies such as robust, adaptive control, smart structures, advanced multi-sensor data fusion, composite manufacturing and other cost-saving advancements that promise to revolutionize our access to space by reducing the cost of engineering development and shortening the time from mission conception to mission execution. We require research to unlock the potential in these new technologies to make them relevant for future space missions.

Spacecraft navigation and controls engineers are accustomed to extracting data from multiple sources in an effort to accurately determine a spacecraft's attitude, attitude rates and orbital parameters [35]. Star positions, gyros, accelerometers, sun sensors, earth horizon sensors, magnetometers and GPS receivers are all common sensors used for spacecraft navigation and control.

The purpose of this research is to investigate new ways to obtain more performance out of less equipment, thereby reducing the overall cost and complexity of satellite missions. Specifically, by extracting more information from star trackers, satellite designers may be able to one day improve the navigation (both attitude and orbit) solution while simultaneously reducing the cadre of sensors required to complete the mission.

The Problem of Space Debris

As space commerce continues to grow, so does the density of space assets in "popular" orbits (low earth orbit, polar orbits, sun synchronous orbits and geostationary orbits) [36]. These assets mostly include spent rocket bodies and satellites (many have been inactive for years or decades). Similar to the meticulous measurements astronomers take to map the location of stars in the sky [37], space researchers and military organizations measure and track orbital parameters of most RSOs larger than 5 cm in diameter [38,39].

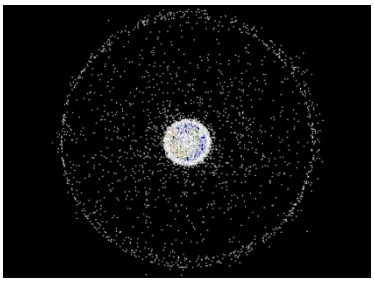

Figure 1: High-Level Distribution of RSOs, (Credit: NASA/JSC/Orbital Debris Program Office).

Star Trackers for RSO Detection and Navigation

As the population of space debris has grown, star tracking algorithms have had to become increasingly intelligent to reject "false" star images arising from glinting space objects. These algorithms attempt to identify non-star images and actively reject them prior to forwarding the starfield image to the guide star catalog correlator for identification.

Recent research by York University and Magellan Aerospace [40] has made progress towards the opposite problem – one of using star trackers as a tool for detecting and cataloging RSOs. With the possibility now of positively identifying RSOs with star trackers, this research addresses the feasibility of using those RSO observations as a means of navigating.

On a small scale, the concept of using other space assets to assist in navigation is not new. As part of previous research at MIT, Dr. Ferguson studied ways in which a fleet of cooperative spacecraft could decentralize their fleet state estimation (orbital determination) using GPS and local transmitters that measured the distance and velocity (using Doppler measurements) between every pair of spacecraft in the fleet [41,42].

Using star tracker measurements from nearby space debris opens up a new avenue of navigation. Unlike a star tracker that only detects stars assumed to be "at infinity", the position of an RSO with respect to the sensor on the satellite changes as a function of the orbital position. This orbital position as well as attitude dependence means that, theoretically, the star tracker could provide orbital knowledge in addition to the traditional attitude knowledge typically assumed for star trackers. This paper studies this geometry, in combination with a combined position and attitude Extended Kalman Filter (EKF) to assess the feasibility of such an estimator.

PROBLEM FORMULATION

First, let us explore a simplified two-dimensional model of the relationship between an observing satellite and an RSO or other detectable object.

Consider an observer moving in a circular path (or orbit) and a fixed object as shown in Figure 2. Our goal in this work is to estimate the position, attitude and rates of the observer using angular measurements between the observer and various objects.

The observer has a position of (x_{obs},,y_{obs}) and an attitude angle of φ. The observer detects the relative angle θ between its local frame of reference and the fixed object. We assume that the observer has access to a database of objects and that we know the position of the object. Let the global position of the object be (x_i,y_i) and let (Δx,Δy) denote the relative position of the object with respect to the observer.

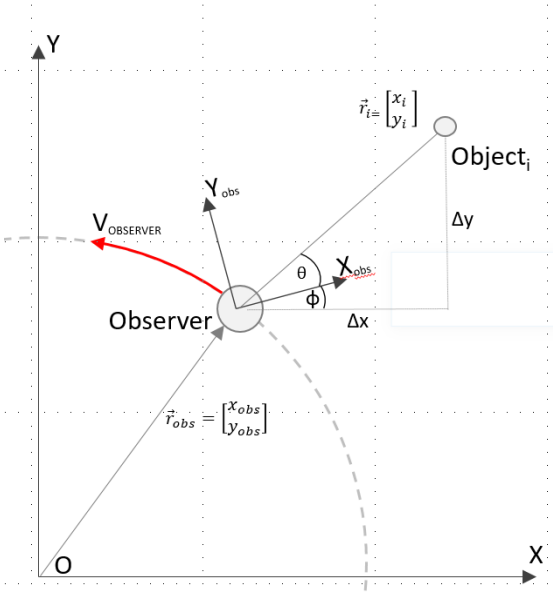

Figure 2: An Observer in a Circular Orbit Detecting the Angle between its Internal Reference Frame and an External Point i

From Figure 2 we note that:

$$tan(\theta + \varphi) = \frac{y_i - y_{observer}}{x_i - x_{observer}} \tag{1}$$

Assuming that the position of the observed object is known, then we can express the observed angle measurement (z) as a function of the observed object's position and the observer's position:

$$z = tan^{-1}\left[\frac{y_i - y_{observer}}{x_i - x_{observer}}\right] - \varphi \tag{2}$$

It should be noted that this model includes several simplifications: the model only considers movement in two dimensions and rotation in one dimension, the observer is in a circular orbit and the observed object is fixed, and the observed object is continually observable.

OBSERVABILITY ANALYSIS

With our intent to establish the feasibility of a combined position and attitude estimator using a combination of star and RSO observations, we would like to investigate the observability of position and attitude states resulting from a collection of measurements.

Letting *i* denote a singular angle measurement from an object (a star or an RSO), we can define a partial observation matrix (one including only the x position state and the attitude angle state) as:

$$H_i = \begin{bmatrix} \frac{\partial z}{\partial x} & \frac{\partial z}{\partial \varphi} \end{bmatrix} = \begin{bmatrix} a & -1 \end{bmatrix} \tag{3}$$

Where

$$a = \frac{y_i - x_{obs}}{{x_i}^2 + {y_i}^2 + {x_{obs}}^2 + {x_{obs}}^2 - 2x_i x_{obs} - 2y_i y_{obs}} \tag{4}$$

We recognize that:

$$|r_{obs}|^2 = {x_{obs}}^2 + {x_{obs}}^2 \tag{5a}$$

$$|r_i|^2 = {x_i}^2 + {x_i}^2 \tag{5b}$$

are the squared magnitudes of the positions of the observer and the observed object respectively. Substituting this relationship into the above yields:

$$a = \frac{y_i - x_{obs}}{|r_i|^2 + |r_{obs}|^2 - 2x_i x_{obs} - 2y_i y_{obs}} \tag{6}$$

Rearranging the above (dividing the top and bottom by the square of the position magnitude of the object):

$$a = \frac{\frac{y_i}{|r_i|^2} - \frac{x_{obs}}{|r_i|^2}}{1 + \frac{|r_{obs}|^2}{|r_i|^2} - 2\frac{x_i x_{obs}}{|r_i|^2} - 2\frac{y_i y_{obs}}{|r_i|^2}} \tag{7}$$

For cases where the observed object is a star, we can approximate this distance ($|r_i|^2$) as ∞. In this case, we can immediately see that for measurements from stars, the quantity *a* vanishes, but for RSOs, *a* is non-zero.

In our simplified example, if we consider one star measurement and one RSO measurement, we then have a two-row H matrix

$$H = \begin{bmatrix} a_{star} & -1 \\ a_{RSO} & -1 \end{bmatrix} \approx \begin{bmatrix} 0 & -1 \\ a_{RSO} & -1 \end{bmatrix} \tag{8}$$

It is well-understood in the field of estimation that the invertibility of $H^T H$ describes the instantaneous observability of our measurements to our state. Looking closer at this, we have:

$$H^T H \approx \begin{bmatrix} 0 & a_{RSO} \\ -1 & -1 \end{bmatrix} \begin{bmatrix} 0 & -1 \\ a_{RSO} & -1 \end{bmatrix} = \begin{bmatrix} {a_{RSO}}^2 & -a_{RSO} \\ -a_{RSO} & 2 \end{bmatrix} \tag{9}$$

By inspection, we can see that the above matrix will be invertible for any non-zero a_{RSO} (with a reasonable magnitude).

While reasonably simple, this analysis lends credibility to the claim that a combination of observations from both near and far objects will lead to sufficient observability in position and attitude simultaneously. The following section presents a filter for estimating position and attitude from star and RSO observations.

NAVIGATION FILTER DESIGN

The authors developed a filter based on the previously described orbital model to determine if an observer's state can be accurately estimated using the previously derived measurement equation (equation 2). We chose to use an extended Kalman filter (EKF) per the methods of [43] as an EKF is capable of linearizing our nonlinear state estimate.

First, the observer's state vector x was defined, as seen below, included both the observers position and velocity in x and y as well as the observers attitude φ and rotational velocity.

$$\dot{X} = \begin{bmatrix} x \\ y \\ \dot{x} \\ \dot{y} \\ \varphi \\ \dot{\varphi} \end{bmatrix} \tag{10}$$

However, as we have chosen to use Cartesian coordinates to describe the observer's dynamics, the observer's angular acceleration in x and y is a function of its previous position:

$$a_x(t) = x_{t-1}\vec{r}\omega^2 \left[\frac{\vec{r}}{|\vec{r}|}\right]$$

$$a_y(t) = y_{t-1}\vec{r}\omega^2 \left[\frac{\vec{r}}{|\vec{r}|}\right] \tag{11a, 11b}$$

Neglecting process noise w, this results in the nonlinear system of equations seen below:

$$X_{k+1} = f(X_k, u_k, w_k) = \begin{bmatrix} x + \dot{x}\Delta t + \frac{\Delta t^2}{2}\left[\frac{-x\omega^2\vec{r}^2}{|\vec{r}|}\right] \\ y + \dot{y}\Delta t + \frac{\Delta t^2}{2}\left[\frac{-y\omega^2\vec{r}^2}{|\vec{r}|}\right] \\ \dot{x} + \frac{\Delta t}{m}\left[\frac{-x\omega^2\vec{r}^2}{|\vec{r}|}\right] \\ \dot{y} + \frac{\Delta t}{m}\left[\frac{-y\omega^2\vec{r}^2}{|\vec{r}|}\right] \\ \varphi + \dot{\varphi}\Delta t + \Delta t^2 T\cos(k\Delta t) \\ \dot{\varphi} + \frac{\Delta t}{I}T\cos(k\Delta t) \end{bmatrix} \quad (12)$$

Where m is the observer's mass, I is its inertia, T is the torque imparted onto the observer, r is the observer's orbital radius, k is the current time step, and Δt is the sample time.

As simplifications, mass m and particle inertia I were assumed to be unity. An arbitrary torque of 0.01 Nm and time steps of 0.05 s were used.

A process noise Q was included as a random normal standard deviation of amplitude 0.0001 with a standard deviation equal to the square root of the amplitude. This was multiplied by matrix W where:

$$\widehat{W} = \begin{bmatrix} 0 \\ 0 \\ 1 \\ 1 \\ 0 \\ 1 \end{bmatrix} \quad (13)$$

After these observer dynamics were created, 'true' measurements were taken for each observed object and timestep using the previously described measurement equation (Equation 2). Sample measurements were obtained by taking the random normal standard deviation of these true measurements with a standard deviation of 0.0001 radians. Note that the EKF formulation requires a linearized measurement equation using similar terms to Equation 3.

SIMULATION RESULTS

As described above, the purpose of this work is to investigate the feasibility of combined position and attitude determination using a combination of star and orbital space object observations. To that end, this section describes a set of simulations that demonstrate the utility of such an estimator in several different scenarios.

All tests were performed using time steps of 0.05s for an observer in a 400 km circular orbit. Except for Test 7, the observer's orbital velocity is 7672 m/s.

Test 1: Infinitely Far Objects and Attitude Estimation

First, we verify the known result that star tracker measurements of stars can support attitude-only estimation. This test mimics the way that typical star trackers are used and was performed using four equally spaced objects 1,600 light years (effectively an infinite distance) away from the observer. For this initial test, the state model included only the attitude element and a simplified measurement equation was used.

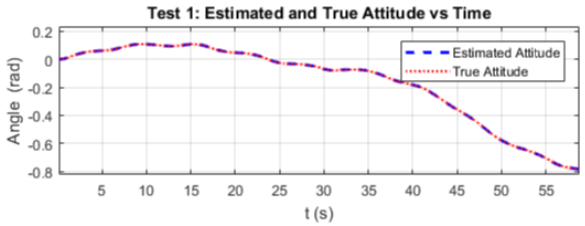

(a)

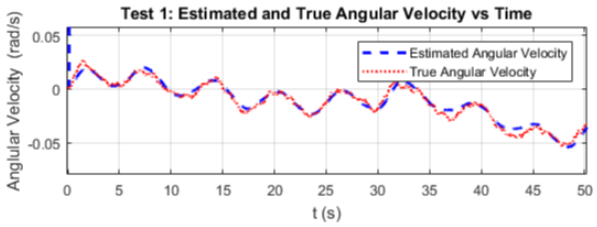

(b)

Figure 3: Observer Attitude and Angular Velocity with Respect to Time.

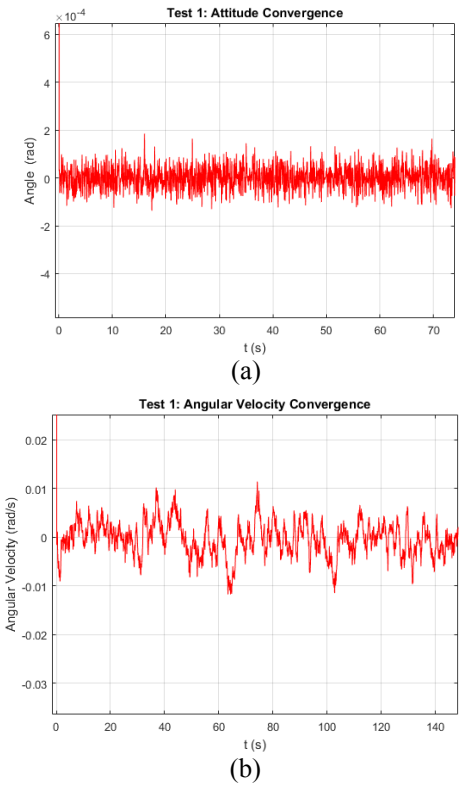

Figure 4: Observer Attitude (a) and Angular Velocity (b) Convergence with Respect to Time.

As expected, the filter quickly converges on an accurate attitude estimate.

Test 2: Infinitely Far Objects and Position Estimation

Next, we re-ran the same test-set as in Test 1 but using the full state model (including position as well as attitude status) and associated measurement equation. This time while the filter was able to quickly converge on an accurate attitude estimate, the filter was incapable of determining the observer's position or velocity, as seen in Figure 5a. This is expected since star trackers cannot provide position estimates from star measurements alone (per our analysis above).

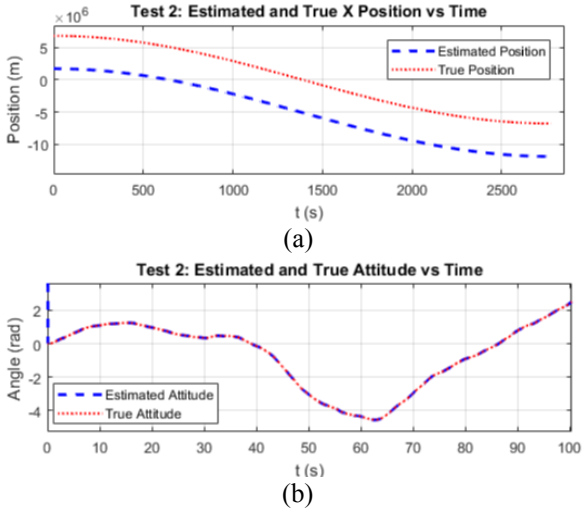

Figure 5: True and Estimated Observer Attitude and Angular Velocity over Time When Measuring Position and Observing Four Infinitely Far Points.

Test 3: Position and Attitude Estimation with Both Infinitely far and Near Objects

For the third test, we added three additional distantly spaced objects at 30,000 km altitudes to represent objects near geostationary orbit. With these additional objects, the filter quickly converged on accurate attitude and accurate position estimates, as seen in Figure 6 and Figure 7, within approximately 0.36 orbits. This confirms our hypothesis that RSO observations could enable star trackers to estimate position as well as attitude.

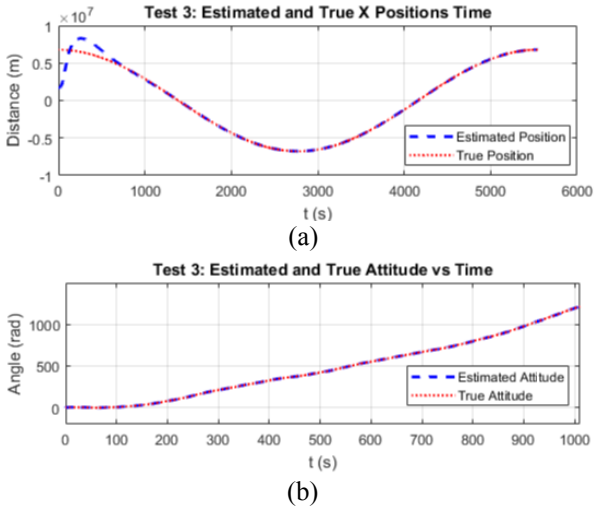

Figure 6: True and Estimated Observer Position (a) and Attitude (b) over Time When Measuring Four Infinitely Far Objects and Three Objects at 30,000 km.

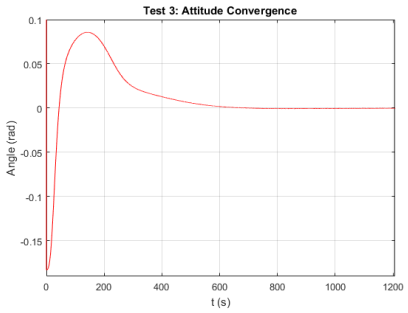

(a)

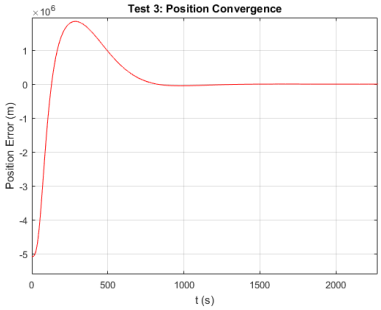

(b)

Figure 7: Attitude (a) and Position (b) Convergence When Observing Four Infinitely Far Objects and Three Objects at 30,000 Km.

Test 4: Position and Attitude Estimation with Infinitely far, Near, and Very Near Objects

For the fourth test, measuring the effect of additional closer objects, we inserted three distantly spaced objects at 8,000 km altitudes. As shown in Figures 8 and 9, the position estimate converged within 0.24 orbits, confirming that more observations from near objects help improve the filter's performance.

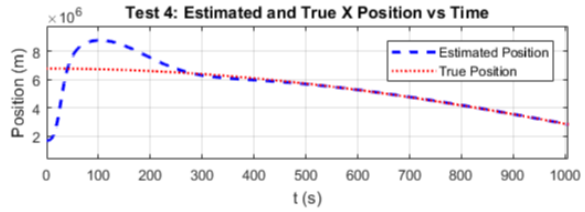

(a)

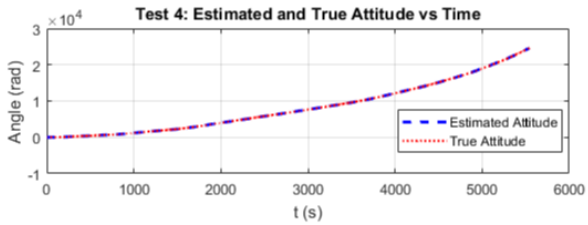

(b)

Figure 8: True and Estimated Observer Position (a) and Attitude (b) over Time When Observing Four Infinitely Far Objects, Three Objects at 30,000 Km, and Three Objects at 8,000 Km.

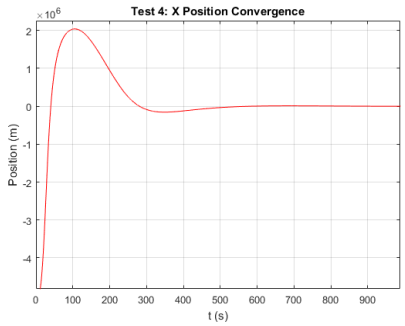

(a)

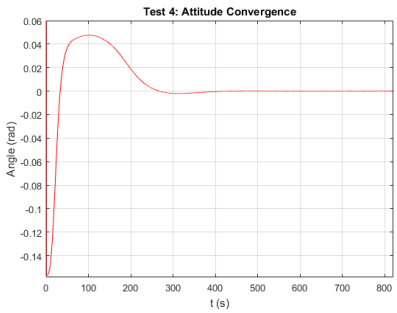

(b)

Figure 9: Observer X Position (a) and Attitude (b) Convergence When Observing Four Infinitely Far Objects, Three Objects at 30,000 km, and Three Objects at 8,000 km.

Test 5: Position and Attitude Estimation with Only Near and Very Near Objects

Next, the infinitely far objects (stars) were removed to test the filter's ability to track position and attitude using only near objects. The system was run using the same three objects at 30,000 km and three at 8,000 km. Figure 10 below shows the observer's estimated and true attitude and angular velocity as well as position in x and y over time.

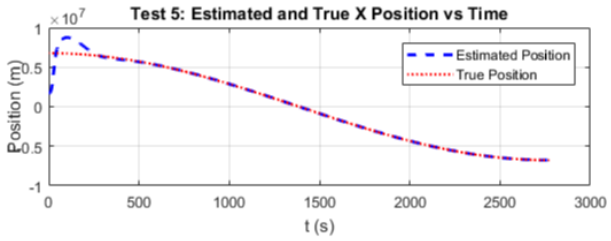

(a)

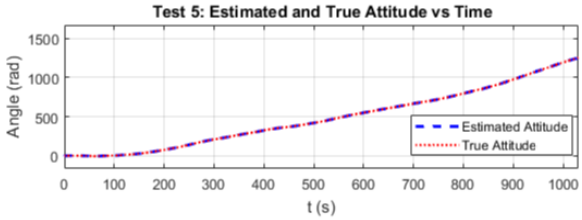

(b)

Figure 10: True and Estimated Observer Position (a) and Attitude (b) Over Time When Observing Three Objects at 30,000 km and Three Objects at 8,000 km.

Both attitude and positional estimates converged, with attitude converging within 0.16 orbits and position converging within 0.46 orbits, as seen below in Figure 11.

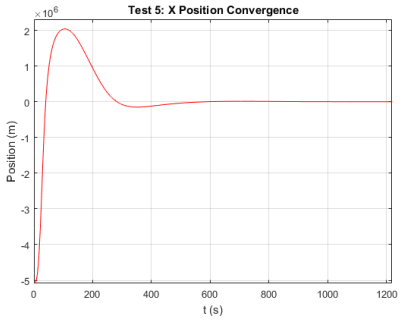

(a)

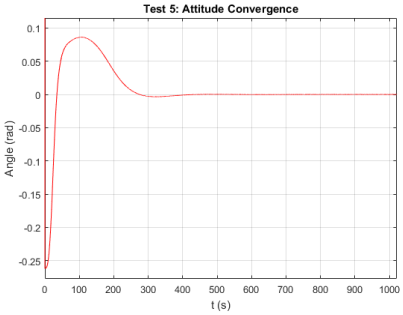

(b)

Figure 11: Observer X Position (a) and Attitude (b) Convergence When Observing Three Objects at 30,000 km and Three Objects at 8,000 km.

DISCUSSION

As seen in Figures 3-11, the filter is capable of consistently converging on an accurate estimate of the observer's attitude and position for a wide variety of object quantities, distances, and locations. Increasing the number of objects and/or decreasing their distance to the observer improves the filter's convergence.

As seen by the second test, as object distance approaches infinity, the filter can provide an accurate attitude estimate but is not able to converge on an accurate positional estimate. This is to be expected by observing the relationship between object and observer positions in the measurement equation. As the target object position approaches infinity, the difference between the observer and object positions becomes a constant equal to the arctangent of the object's x and y positions:

$$\theta = \lim_{x_i, y_i \to \infty} \left[tan^{-1} \left[\frac{y_i - y_{observer}}{x_i - x_{observer}} \right] - \varphi \right]$$

$$\hat{=} tan^{-1} \left[\frac{y_i}{x_i} \right] - \varphi \hat{=} \mathrm{c} \ -\varphi \qquad (14)$$

As a result of the above relation, the position of the observer becomes unobservable for far away objects. Fortunately, the second test demonstrated that objects as far away as geostationary orbit provide enough observability to render a viable position estimate.

The third test shows that the filter is capable of converging with relatively few close objects and, by observing the difference between the third and fourth test, we can see that increasing the quantity of objects reduces the convergence time and estimate error.

Similarly, by comparing tests three and five, we can see that the filter is not only capable of functioning without infinitely far reference objects but that the filter converges faster when we replace the far objects with the same number of near objects. This is also to be expected as near objects provide the filter with information on both the observer's attitude and position.

Finally, to explore the role dynamics play (through constantly changing geometries) on the filter's convergence time, we ran a series of tests using near and a combination of near and infinitely far objects with varying orbital velocities. Three distantly spaced objects at 30,000 km and three distantly spaced objects at 8,000 km were used for the near-only case while four infinitely far objects were added for the combined case. These tests used the previous velocity of 7672 km/s as

well as 767.2 km/s, 76.72 km/s, 7.67 km/s, 0.76 km/s and 0.076 km/s. Figure 12 summarizes the resulting relationship between orbital velocity and convergence time for each case.

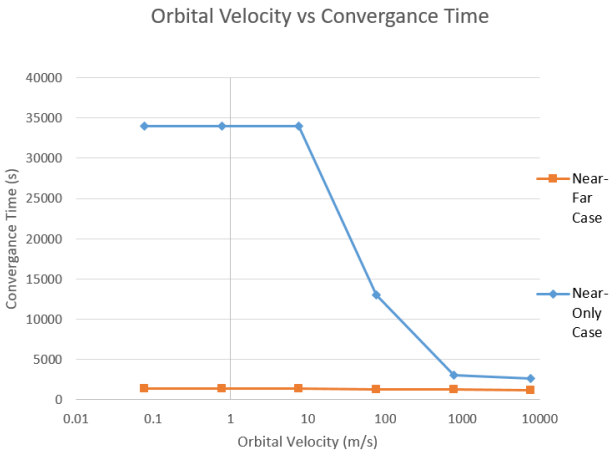

Figure 12: Orbital Velocity vs X Position Convergence Time

As demonstrated by Figure 12, decreasing the observer's orbital velocity increases convergence time significantly when near objects are visible, to a limit of approximately 3.4×10^4 seconds, but has little effect on convergence time when far objects are present in the measurements. This confirms that the filter requires measurement motion in order to differentiate between attitude and position data in the measurements when no far objects are in view. This is expected since the far objects provide nearly pure angle information, which the filter can use to disambiguate the position and attitude data from the near object measurements. Note, however, that even while using only near objects, the filter still converges, albeit slowly due to the filter requiring relative object / observer motion for observability.

This filter achieves promising results, as demonstrated by its ability to converge on accurate state estimates for a wide variety of observation scenarios. However, there are many areas in which our model can be improved: converting the system to a full three-dimensional model with quaternions, having both the observer and observed objects move in elliptical orbits, model the observed objects based off of RSO data, and include a field of view mechanism for detecting observations based on commercial star trackers.

Expanding the model into three dimensions is unlikely to have a large effect on the overall effectiveness of the filter, as each observation will include additional state information proportional to the additional degrees of freedom.

We expect that having the observed objects move in RSO-type orbits will increase the effectiveness of our filter since causing the objects to move will increase the variation in distances and velocities between the observer and observed objects. As seen in the varying orbital velocity test, higher relative measurement variation increases the performance of the filter.

Conversely, introducing a star tracker-based measurement model will reduce the effectiveness of the filter as it will reduce the number of detected objects at any given time. Introducing this feature will likely require a higher number of objects to be inserted into the model. However, given the quantity of RSOs currently in orbit, it is likely possible that a sufficient quantity of observations can be achieved.

CONCLUSIONS

This paper has presented the preliminary work towards developing an extended Kalman filter for determining a satellite's position and attitude using RSO observations.

While the dynamics model has included several simplifications, the simulations demonstrate that it is possible to converge on an accurate estimation of an observer's state when provided with accurate data on the state of observed objects. As shown, these estimates converge within a fraction of the observer's orbit with relatively few (≤ 6) observed bodies.

Based on these results, the authors have concluded that position and attitude estimation is possible using RSO observations and will continue this expand on this work to provide more accurate dynamics and measurement models.

ACKNOWLEDGEMENTS

The authors thank the Natural Sciences and Engineering Research Council (NSERC) of Canada and Magellan Aerospace for supporting this research.

References

1. Tapley, B. D., S. Bettadpur, M. Watkins, and C. Reigber (2004), The gravity recovery and climate experiment: Mission overview and early results, Geophys. Res. Lett., 31, L09607, doi:10.1029/2004GL019920.

2. Saps Buchman, C.W.F. Everitt, B. Parkinson, J.P. Turneaure, D. DeBra, D. Bardas, W. Bencze, R. Brumley, D. Gill, G. Gutt, D.H. Gwo, G.M. Keiser, J. Lipa, J. Lockhart, J. Mester, B. Muhlfelder, M. Taber, S. Wang, Y. Xiao, P. Zhou, The Gravity Probe B Relativity Mission, Advances in Space Research, Volume 25, Issue 6, 2000, Pages 1177-1180, ISSN 0273-1177.

3. Bernath, P. F., et al. (2005), Atmospheric Chemistry Experiment (ACE): Mission overview, Geophys. Res. Lett., 32, L15S01, doi:10.1029/2005GL022386.

4. A.W. Yau and H. G. James. Scientific Objectives of the Canadian CASSIOPE Enhanced Polar Outflow Probe (e-POP) Small Satellite Mission. Chapter in "The Sun, the Solar Wind, and the Heliosphere", Volume 4 in the series IAGA Special Sopron Book Series pp 355 – 364. December 10, 2010.

5. Christensen, A. B., et al. (2003), Initial observations with the Global Ultraviolet Imager (GUVI) in the NASA TIMED satellite mission, J. Geophys. Res., 108, 1451, doi:10.1029/2003JA009918, A12.

6. A. G. Davies, S. Chien, V. Baker, T. Doggett, J. Dohm, R. Greeley, et al., "Monitoring active volcanism with the Autonomous Sciencecraft Experiment on EO-1", *Remote Sens. Environ.*, vol. 101, no. 4, pp. 427-446, 2006.

7. A. G. Davies, S. Chien, R. Wright, A. Miklius, P. Kyle, M. Welsh, et al., "Sensor web enables rapid response to volcanic activity", *EOS*, vol. 87, no. 1, 2006.

8. B. T. San and S. M. Lutfi, "Evaluation of cross-track illumination in EO-1 Hyperion imagery for lithological mapping", *Int. J. Remote Sens.*, vol. 32, no. 22, pp. 7873-7889, 2011.

9. Berry, P. A. M., J. D. Garlick, J. A. Freeman, and E. L. Mathers (2005), Global inland water monitoring from multi-mission altimetry, Geophys. Res. Lett., 32, L16401, doi:10.1029/2005GL022814.

10. C. Donlon, B. Berruti, A. Buongiorno, M.-H. Ferreira, P. Féménias, J. Frerick, P. Goryl, U. Klein, H. Laur, C. Mavrocordatos, J. Nieke, H. Rebhan, B. Seitz, J. Stroede, R. Sciarra, The Global Monitoring for Environment and Security (GMES) Sentinel-3 mission, Remote Sensing of Environment, Volume 120, 15 May 2012, Pages 37-57, ISSN 0034-4257.

11. S. Michel, P. Gamet and M. J. Lefevre-Fonollosa, "HYPXIM — A hyperspectral satellite defined for science, security and defence users," *2011 3rd Workshop on Hyperspectral Image and Signal Processing: Evolution in Remote Sensing (WHISPERS)*, Lisbon, 2011, pp. 1-4. doi: 10.1109/WHISPERS.2011.6080864.

12. Smith, Patrick L., Leslie A. Wickman, and Inki A. Min. "Future Space System Support to US Military Operations in an Ice-Free Arctic: Broadband Satellite Communications Considerations." *AIAA Proceedings*. 2009.

13. Garand, Louis, et al. "THE POLAR COMMUNICATIONS AND WEATHER." *PHYSICS IN CANADA* 70.4 (2014).

14. Karna, Y. K. "Mapping above ground carbon using worldview satellite image and lidar data in relationship with tree diversity of forests." *The Netherlands: Master's thesis, Faculty of Geoinformation Science and Earth Observation, University of Twente* (2012).

15. Eckert, Sandra. "Improved forest biomass and carbon estimations using texture measures from WorldView-2 satellite data." *Remote sensing* 4.4 (2012): 810-829.

16. Williams, Darrel L., Samuel Goward, and Terry Arvidson. "Landsat." *Photogrammetric Engineering & Remote Sensing* 72.10 (2006): 1171-1178.

17. Chander, Gyanesh, Brian L. Markham, and Dennis L. Helder. "Summary of current radiometric calibration coefficients for Landsat MSS, TM, ETM+, and EO-1 ALI sensors." *Remote sensing of environment* 113.5 (2009): 893-903.

18. Entekhabi, Dara, et al. "The soil moisture active passive (SMAP) mission." *Proceedings of the IEEE* 98.5 (2010): 704-716.

19. Flett, Dean, Yves Crevier, and Ralph Girard. "The RADARSAT constellation mission: Meeting the government of Canada's needs and requirements."*2009 IEEE International Geoscience and Remote Sensing Symposium*. Vol. 2. IEEE, 2009.

20. Meinecke, G., V. Ratmeyer, and G. Wefer. "Bi-directional communication into the deep ocean based on ORBCOMM satellite transmission and acoustic underwater communication." *OCEANS'99 MTS/IEEE. Riding the Crest into the 21st Century*. Vol. 3. IEEE, 1999.

21. Breiling, M., et al. "LTE backhauling over MEO-satellites." 2014 7th Advanced Satellite Multimedia Systems Conference and the 13th Signal Processing for Space Communications Workshop (ASMS/SPSC). IEEE, 2014.

22. Teles, J., M. V. Samii, and C. E. Doll. "Overview of TDRSS." *Advances in Space Research* 16.12 (1995): 67-76.

23. Perillan, Luis B., William R. Schnicke, and

Edward A. Faine. "Intelsat VI system planning." *COMSAT Technical Review* 20 (1990): 247-269.

24. Grocott, Simon, Robert Zee, and Jaymie Matthews. "The MOST microsatellite mission: one year in orbit." From the Proceedings of the 2004 Small Satellite Conference, Logan Utah, (2004).
25. Laurin, Denis, et al. "NEOSSat: A Canadian small space telescope for near Earth asteroid detection." *SPIE Astronomical Telescopes+ Instrumentation*. International Society for Optics and Photonics, 2008.
26. Polidan, Ronald S. "Hubble Space Telescope overview." *29th AIAA Aerospace Sciences Meeting*. Vol. 1. 1991.
27. Gardner, Jonathan P., et al. "The James Webb Space Telescope." *Space Science Reviews* 123.4 (2006): 485-606.
28. Weisskopf, Martin C., et al. "Chandra X-ray Observatory (CXO): overview." *Astronomical Telescopes and Instrumentation*. International Society for Optics and Photonics, 2000.
29. Crouch, Geoffrey I. "The market for space tourism: early indications." *Journal of Travel Research* 40.2 (2001): 213-219.
30. Isozaki, Kohki, et al. "Considerations on vehicle design criteria for space tourism." *Acta Astronautica* 37 (1995): 223-237.
31. Webber, Derek. "Space tourism: Its history, future and importance." *Acta Astronautica* 92.2 (2013): 138-143.
32. Loizou, John. "Turning space tourism into commercial reality." *Space Policy*22.4 (2006): 289-290.
33. Sonter, Mark Joseph. "The technical and economic feasibility of mining the near-earth asteroids." *Acta Astronautica* 41.4 (1997): 637-647.
34. Feinman, Matthew. "Mining the Final Frontier: Keeping Earth's Asteroid Mining Ventures from Becoming the Next Gold Rush." *Pitt. J. Tech. L. & Pol'y*14 (2013): 202.
35. Lefferts, Ern J., F. Landis Markley, and Malcolm D. Shuster. "Kalman filtering for spacecraft attitude estimation." *Journal of Guidance, Control, and Dynamics* 5.5 (1982): 417-429.
36. Liou, Jer-Chyi, et al. "The new NASA orbital debris engineering model ORDEM2000." *Space Debris*, Vol 473, 2001.
37. Lasker, Barry M., et al. "The second-generation guide star catalog: description and properties." *The Astronomical Journal* 136.2 (2008): 735.
38. Maskell, Paul, and Lorne Oram. "Sapphire: Canada's answer to space-based surveillance of orbital objects." *Advanced Maui Optical and Space Surveillance Conference*. 2008.
39. Anheier, Norman C., and C. Chen. *A New Approach to Space Situational Awareness using Small Ground-Based Telescopes*. No. PNNL-23994. Pacific Northwest National Laboratory (PNNL), Richland, WA (US), 2014.
40. Clemens, S., Lee, R., Harrison, P., "Resident Space Object Detection Using Commercial off the Shelf Star Trackers – Preliminary Results of RSO Detection Simulator", poster presentation, CASI ASTRO 2018, May 2018.
41. C.-W. Park, P. Ferguson, N. Pohlman, and J. P. How. Decentralized relative navigation for formation flying spacecraft using augmented CDGPS. In Proceedings of Institute of Navigation GPS Conference, Salt Lake City, UT, September 2001.
42. P. Ferguson and J. How. Decentralized estimation algorithms for formation flying spacecraft. In Proceedings of AIAA Guidance, Navigation and Control Conference, August 2003.
43. A. Gelb. Applied optimal estimation. MIT press, 1974.